ANALYSIS OF GAS-COOLED FAST REACTOR SHIELD DESIGNS*

D. E. Bartine and L. R. Williams
Oak Ridge National Laboratory
Oak Ridge, Tennessee, USA

ABSTRACT

In its shielding program for the Gas-Cooled Fast Reactor (GCFR) as conceived by General Atomic, Oak Ridge National Laboratory has developed an advanced shielding analysis system that incorporates the latest analysis techniques for converging to a shield design compatible with other design parameters such as cooling and structural requirements or material compatibility. Basically the system consists in applying the various techniques in a logical sequence to a given design, thereby generating a large body of data to serve as an information base for subsequent redesign.

As an illustration, this system is applied to successive typical models for the GCFR, resulting in a reduction in the thickness of the radial shield and redesign of the lower shield region. In principle, the design-analysis-redesign iterations would continue until they converge upon an acceptable configuration.

*Research sponsored by the U. S. Department of Energy under Contract W-7405-eng-26 with the Union Carbide Corporation.

1. Introduction

The ORNL methods and codes currently available for shielding analyses are listed in Table 1. They include codes with which radiation transport throughout the reactor-shield system can be calculated in one, two, or three dimensions, both in the forward mode and in the adjoint mode; a technique for coupling two- and three-dimensional transport calculations at a common boundary; a channel-theory analysis technique which allows a determination of the channels in space through which the important radiation particles travel; sensitivity analysis methods for determining the sensitivity of the one- or two-dimensional transport calculations to the cross sections used in them; and an uncertainty analysis system which allows a determination of the uncertainty in the calculated response due to uncertainties associated with the nuclear data used in the calculations.

In a typical application of these techniques to the GCFR, the first step is a discrete ordinates radiation transport calculation for a two-dimensional model of the reactor-shield system. The resulting neutron and gamma-ray fluxes are then converted to isoplots for the responses of concern (radiation damage, heating, etc.), and these are used to locate regions in the system at which those responses are higher than allowed by predetermined constraints. Next, adjoint calculations are performed for the regions of concern, and the resulting adjoint fluxes, together with the forward fluxes, are used in channel-theory calculations to determine the physical paths followed by the particles traveling from the core to those regions. In addition, the adjoint and forward fluxes are used in sensitivity calculations to determine the importance of the cross sections used in the transport calculations as functions of the shield materials and particle energies. Finally, the sensitivity results are utilized in the form of linear perturbation theory to predict the effect of changes in the shield composition and position on the various responses.

In some cases transport calculations for specific regions of the system are calculated in three dimensions, and the results are coupled to the two-dimensional calculations of adjacent or surrounding regions. The three-dimensional calculations are usually limited to regions that

have complicated geometries difficult to describe in two dimensions. However, usually two-dimensional calculations are also performed for these regions so that by comparison with the three-dimensional calculations the adequacy of two-dimensional representations of three-dimensional problems can be determined. Also, on occasion the two-dimensional descriptions as such are to represent "worst-case" situations for the region in question and thereby to set upper limits on the radiation transport through the region. And, of course, prototypic or semiprototypic experiments are sometimes performed to determine geometric effects and to investigate techniques for modeling complicated geometries.[1]

2. Calculations for an Initial Design

The shield analysis system described above was applied to an initial GCFR calculational model shown in Fig. 1. This paper is concerned with the neutrons that leave the reactor core in the downward direction, heading toward the lower deck. These neutrons may reach the prestressed concrete reactor vessel (PCRV) by streaming around the lower end of the radial outer shield, by penetrating through the wraparound shield, or by streaming into the lower axial helium channel. In these first calculations the purpose was to determine the fluxes of the neutrons that followed each of these paths to the liner and the resulting radiation heating produced at each location. The quantities were then to be compared with the maximum allowable values of each that were recommended.

The calculations were performed in two-dimensional geometry with the discrete ordinates code DOT and a P_3 expansion of a cross-section set including 51 neutron groups and 25 gamma-ray groups.

The results from the calculation based on the laminated shield model are shown in the first part of Table 2 (Initial Model results). For this model the maximum values above the wraparound region occur just above the wraparound shield. The recommended restraints should not be viewed as being firm.

The initial model calculations revealed that the high-energy neutron flux along the PCRV liner is not a problem, but that the thermal-neutron flux exceeds the recommended restraint at all locations. Neither does gamma-ray heating in the liner appear to be a problem, although it does

exceed the constraint above the wraparound region. The heating in the lubricant for the tendons compressing the PCRV is excessive, however, especially above the wraparound region.

Isoplots of the thermal-neutron fluxes calculated for the initial model are shown in Fig. 2. The isoflux contours show the streaming up the outside of the outer radial shield and indicate that the maximum contour extends above the wraparound shield, its value being 7×10^{10} neutrons $cm^2 \cdot sec^{-1}$. It appeared that with the addition of B_4C as a thermal poison and proper shield redesign, a reduction in the radial dimension of the radial dimension of the reactor cavity might be possible.

3. Calculations for Revised Design

A study of potential revised radial shield designs reduced the outer radial shield thickness by 1 ft. The revised outer shield consisted of an 18-cm-thick graphite layer followed by an 18-cm-thick graphite-B_4C mixture (about 19% B_4C by weight) and a 5-cm-thick stainless steel 304 region. A corresponding reduction in the radius of the PCRV was also made.

Calculations for the revised design shown in the second part of Table 2 reveal that the high-energy neutron flux is still maintained well below the constraint, the maximum fluxes on the PCRV liner occurring this time at a location just below the inner shield. The gamma-ray heating in the liner also remains below the constraint. However, the thermal-neutron flux at the liner is still too high, as is the heating in the tendon lubricant. An isoplot of the thermal-neutron flux included in Fig. 2 (above, right) indicates a high flux level at the lower axial helium channel and wraparound position but a reduced level above the wraparound shield.

A series of adjoint calculations for the revised design were then initiated, including calculations for the thermal-neutron flux levels in the PCRV liner at the lower axial helium channel and wraparound shield, for PCRV gamma-ray heating at the lower axial helium channel, and for the gamma-ray dose in the tendon lubricant at the lower axial helium channel and wraparound shield. The resulting adjoint fluxes were then used, together with the forward fluxes, in the FANG channel-theory code to produce three-dimensional plots of the contributon fluxes,

where a "contributon" is a particle that contributes to the response of interest. Thus, the plots depict the passage of contributing particles from the reactor core to the location where the response has been determined.

A plot showing the pathways taken by the contributons that produce the gamma-ray dose in the tendon lubricant at the wraparound shield level is shown in Fig. 3, where the corner in the lower center of the figure is located just below the reactor core on the axis of the assembly. The plot shows a primary streaming path around the outer shield, the first peak occurring in the helium gap just below the shield. The second peak occurs in the PCRV liner, where thermal neutrons are captured in the iron. The highest peak occurs in the PCRV at the tendon position itself, where thermal-neutron capture in the concrete contributes the major fraction of the dose.

Interpretation of Fig. 3 is aided by the plot shown in Fig. 4. Here the contributons plotted are those responsible for the thermal-neutron fluxes in the liner just above the wraparound shield. This plot primarily indicates the paths of high-energy neutrons to regions where they are thermalized and then transported to the location of interest in the liner.

Additional information on the thermal neutrons and gamma rays in the vicinity of the PCRV liner was obtained from sensitivity studies performed with the VIP code, which also required the forward and adjoint fluxes as input. Table 3 presents the sensitivities calculated for the thermal-neutron flux in the PCRV liner at the wraparound level, where the sensitivity is the predicted change in the flux per percent increase in the macroscopic neutron cross section for the spatial region indicated.

The sensitivity of the gamma-ray dose at the tendon position at the wraparound level to both the neutron macroscopic cross section and the gamma-ray macroscopic cross section of the various spatial regions is given in Table 4, which also shows where the gamma rays contributing to the response are born.

All the above results indicate that the high thermal-neutron fluxes and gamma-ray heating responses at the PCRV liner are attributable to high-energy neutrons being transported to the region and being thermalized and captured there. From this it can be inferred that redesigning the shields between the core and the liner to reduce the neutron flux levels would alleviate the problem.

Since the adjoint and forward calculations were already available for the revised shield design, it was relatively easy to examine possible alterations to the design by using two-dimensional linear perturbation theory. The initial shield layout and the perturbations to it are shown in Fig. 5, and predicted changes in various responses produced by the perturbations are given in Table 5. The perturbations to the shield are as follows:

Region A: $C+B_4C$ replaces C in the first 2.23 cm of the shield.
Region B: C replaces $C+B_4C$ in the first 12.74 cm of original $C+B_4C$ region.
Region C: SS-304 replaces $C-B_4C$ in the last 1.82 cm of original $C+B_4C$ region.
Region D: $C+B_4C$ replaces SS-304 in the last 0.83 cm of the shield.

The results of this study indicate that the thermal-neutron flux and gamma-ray dose and heating are all strongly affected by the boronation of the inner edge of the outer shield (Region A), and that the thermal-neutron flux along the streaming path was dominated by the effects of boronating the outer edge of the outer radial shield (Region D). These results were obtained from linear perturbation theory and therefore only indicate the relative magnitudes of large effects; they do not show actual results from a calculations of a revised design.

4. Calculations for New Revised Design

A new revised design was obtained which represented a more realistic mockup of the lower shielding. The outer borated graphite section of the outer radial shield was removed at its lower end and design changes were made in the stainless steel deck, the wraparound shield, the lower shield, and several other components. The results of DOT two-dimensional

calculations for this new revised design are included in Table 2. They show considerably increased values for the thermal-neutron flux and gamma-ray heating in the tendon lubricant above the wraparound shield region, both large factors above the criteria, thus requiring additional redesign.

ACKNOWLEDGEMENTS

The authors gratefully recognize the extensive shield redesign efforts and many helpful discussions provided by the GCFR Reactor Physics and Shielding Group headed by C. J. Hamilton, especially the efforts of R. Perkins and C. Rowe.

REFERENCES

1. C. O. Slater and M. B. Emmett, "Analysis of a Fuel-Pin Neutron Streaming Experiment to Test Methods for Calculating Neutron Damage to the GCFR Grid Plate," Proceedings of the Fifth International Conference on Reactor Shielding, R. W. Roussin, L. S. Abbott, and D. E. Bartine, Editors, p. 873, Science Press, Princeton (1977).

Table 1. Available Methods and Codes for Shielding Analysis

Transport Calculations:

- Discrete-ordinates (S_n)
  - DOT (two-dimensional)
  - ANISN (one-dimensional)
- Monte Carlo
  - MORSE (three-dimensional)
- Coupled
  - DOT-DOMINO-MORSE

Channel Theory Analysis: FANG

Sensitivity Analysis:

- SWANLAKE (one-dimensional)
- VIP (two-dimensional

Uncertainty Analysis: FORSS

Table 2. Comparison of Calculated Results for Two-Dimensional Models of GCFR

Parameter and Position	Recommended Constraint	Calculational Results: Lower Axial He Channel	Calculational Results: Wraparound Region	Calculational Results: Maximum Above Wraparound Region
Initial Model				
ϕ(E>1 MeV),*PCRV Liner	2 + 9	2.4 + 7	7.1 + 7	5.3 + 7
ϕ(E<2.38 eV),*PCRV Liner	1 + 9	3.7 + 10	3.3 + 10	7.8 + 10
Heating in PCRV (mW/cm^3)	1 + 0	0.7 + 0	1.0 + 0	1.8 + 0
Heating in Tendon Lubricant (rads)	1 - 1	5.5 + 0	7.7 + 0	1.2 + 1
Revised Model				
ϕ(E>1 MeV),*PCRV Liner	2 + 9	9.9 + 7	1.8 + 8	5.0 + 8
ϕ(E<2.38 eV), PCRV Liner	1 + 9	4.6 + 10	8.5 + 9	1.6 + 9
Heating in PCRV (mW/cm^3)	1 + 0	0.9 + 0	0.3 + 0	0.3 + 0
Heating in Tendon Lubricant (rads)	1 - 1	7.1 + 0	4.3 + 0	2.4 + 0
New Revised Model				
ϕ(E>1 MeV),*PCRV Liner	2 + 9	1.5 + 7	2.5 + 8	5.0 + 8
ϕ(E<2.38 eV),*PCRV Liner	1 + 9	3.7 + 10	8.2 + 9	26.4 + 9
Heating in PCRV (mW/cm^3)	1 + 0	0.7 + 0	1.7 + 0	1.2 + 0
Heating in Tendon Lubricant (rads)	1 + 0	0.8 + 0	9.6 + 0	8.1 + 0

*Neutrons $cm^{-2}sec^{-1}$

Table 3. Sensitivity and Origin of Thermal-Neutron Flux at PCRV Liner Above Wraparound Shield

ORNL-DWG 75-13150

SENSITIVITY	% OF RESPONSE DUE TO THERMAL NEUTRON PRODUCTION IN REGION	REGION
−7.28−1	8.225+0	PCRV LINER
−1.85−2	1.089−1	LOWER SHIELD
−7.02−2	1.772−2	GRAPHITE (OUTER SHIELD)
−3.47−2	8.042−6	C+B_4C (OUTER SHIELD)
−1.89	1.389−3	C+B_4C (WRAPAROUND)
−4.66−1	8.216−1	SS_{304} DECK
−5.35−1	9.543+0	SS_{304} (WRAPAROUND)
−3.74−3	1.003−4	SS_{304} (OUTER SHIELD)
3.24−2	77.773	PCRV
−3.977	96.496	

Table 4. Sensitivity and Origin of Gamma-Ray Dose in Tendon Lubricant at Wraparound Shield Level

ORNL-DWG 75-18152

SENSITIVITY			PERCENT OF RESPONSE DUE TO GAMMA PRODUCTION IN ZONE	DESCRIPTION
NEUTRON	GAMMA	TOTAL		
−5.41−2	−1.22−2	−6.63−2	5.416	LOWER SHIELD
−7.79−1	−5.65−2	−8.36−1	5.106	SS DECK
−2.93−1	−2.47−4	−2.93−1	0.0	He COOLANT
−3.29−2	−2.61−3	−3.55−2	8.52−2	OUTER SHIELD GRAPHITE
−3.37−2	−2.62−3	−3.63−2	3.71−5	OUTER SHIELD C+B_4C
−3.17−3	−5.21−3	−8.38−3	2.23−2	OUTER SHIELD SS_{304}
−1.446	−1.89−2	−1.465	2.74−4	B_4C+C WRAPAROUND
−4.97−1	−2.13−1	−7.10−1	3.48−1	SS_{304} WRAPAROUND
−6.35−2	−8.14−2	−1.92−1	9.888	PCRV LINER
−4.21−1	−1.176	−1.598	76.14	PCRV
−3.628	−1.569	−5.245	97.01	

Table 5. Predicted Percent Change in Responses Due to Perturbations in the Revised Shield Design

ORNL-DWG 75-18148

	PREDICTED PERCENT CHANGE				
RESPONSE	REGION A	REGION B	REGION C	REGION D	TOTAL
R1	−1.947+1	5.928−1	1.587−1	−1.693−1	−1.889+1
R2	−6.223+0	5.223−1	5.063−1	−7.059−1	−5.901+0
R3	−6.525+1	2.119+1	8.667+0	−2.679+2	−3.033+2
R4	−1.384+1	4.270−1	2.120−1	−2.578−1	−1.346+1
R5	−3.685+2	5.143−1	3.847−1	−8.432−3	−3.684+2
R6	−3.390+1	5.685−1	1.846−1	−2.029−1	−3.335+1

R1 – E < 2.38 eV FLUX AT LINER AT THE LAHC LEVEL

R2 – E < 2.38 eV FLUX AT LINER AT THE WRAPAROUND REGION.

R3 – E < 2.38 eV FLUX AT LINER AT THE STREAMING PATH POSITION.

R4 – GAMMA DOSE AT TENDON AT THE LAHC LEVEL.

R5 – GAMMA DOSE AT TENDON AT THE WRAPAROUND REGION.

R6 – GAMMA HEATING IN THE PCRV AT THE LAHC LEVEL.

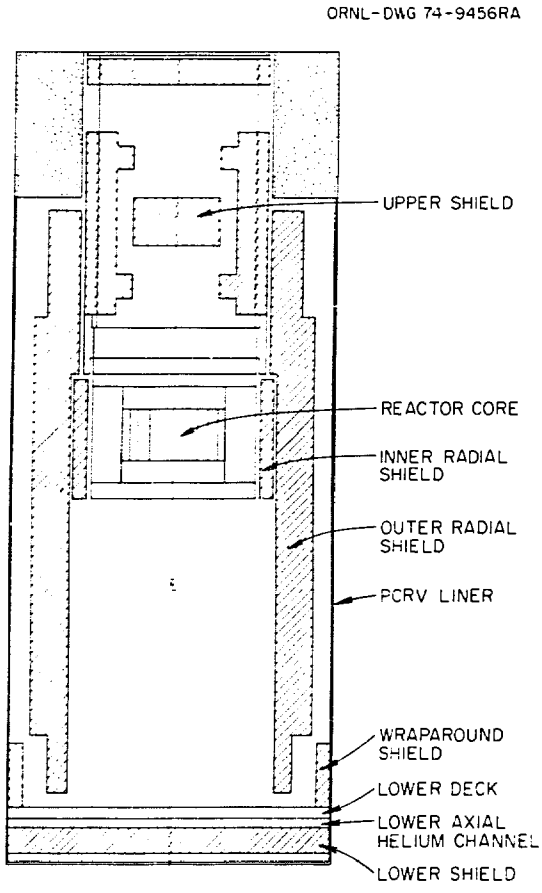

Fig. 1. Two-Dimensional GCFR Calculational Model.

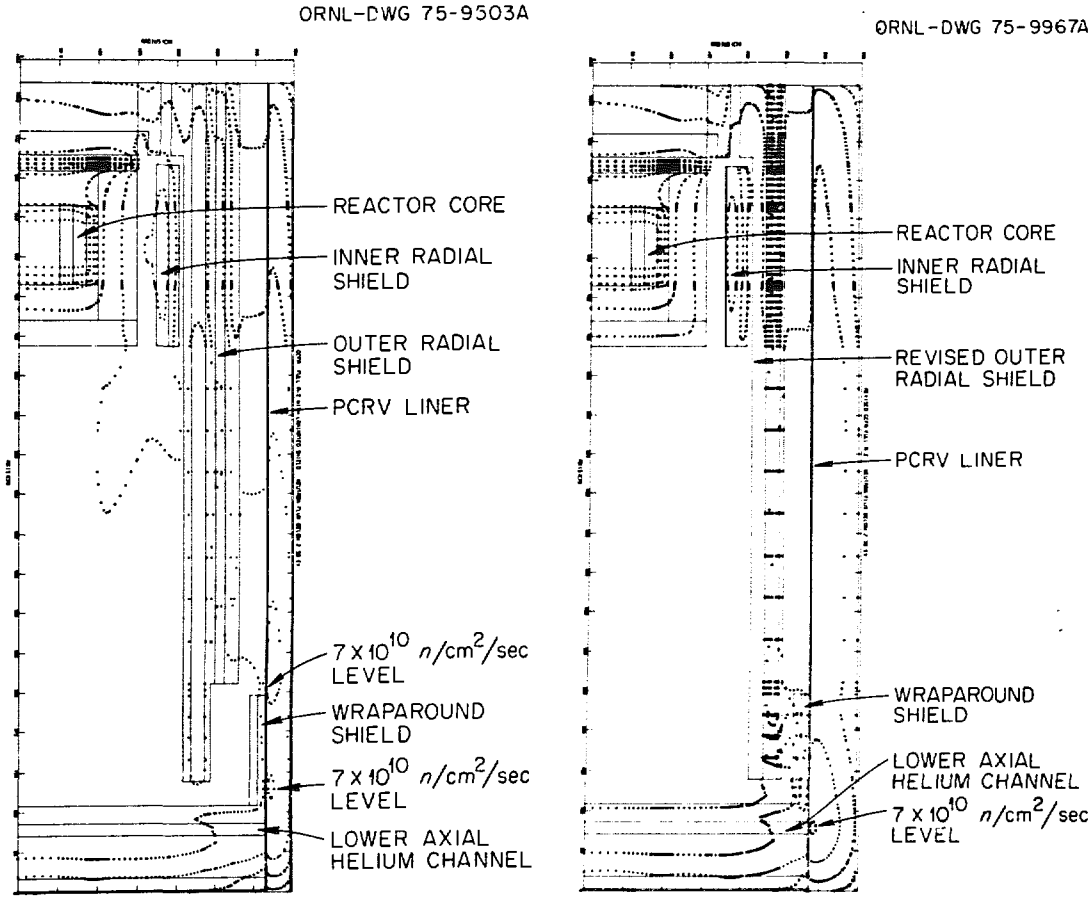

Fig. 2. Isoplots of Thermal-Neutron Fluxes (E<2.38 eV) for Initial (left) and Revised (right) Calculational Models.

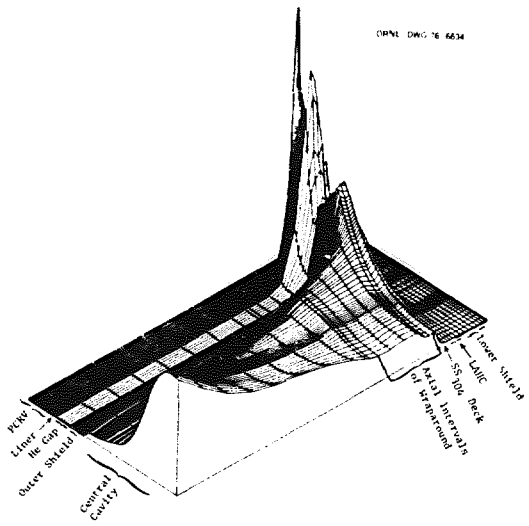

Fig. 3. Plot Showing Pathways of Contributions Producing Gamma-Ray Dose in Tendon Lubricant at Wrap-around Shield Level (Revised Model).

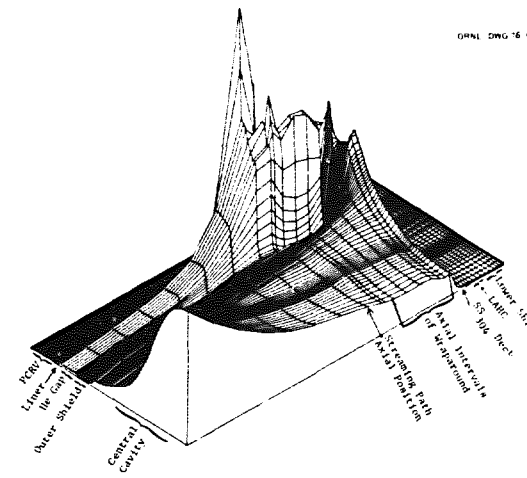

Fig. 4. Plot Showing Pathways of Contributons Producing Thermal-Neutron Fluxes in PCRV Liner Above Wraparound Shield (Revised Model)..

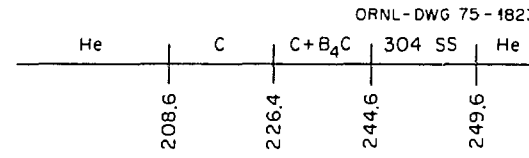

(a) REVISED RADIAL SHIELD LAYOUT.

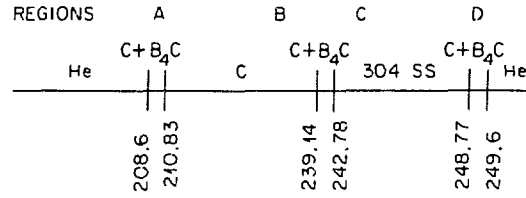

(b) PERTURBATIONS TO REVISED RADIAL SHIELD.

Fig. 5. Revised Radial Shield with Perturbations.